

Modulating properties by light ion irradiation: From novel functional materials to semiconductor power devices

Ye Yuan^{1,†}, Shengqiang Zhou², and Xinxiang Wang^{1,3,†}

¹Songshan Lake Materials Laboratory, Dongguan 523808, China

²Institute of Ion Beam Physics and Material Research, Helmholtz-Zentrum Dresden-Rossendorf, Dresden 01328, Germany

³Dongguan Institute of Optoelectronics, Peking University, Dongguan 523808, China

Abstract: In this review, the application of light ion irradiation is discussed for tailoring novel functional materials and for improving the performance in SiC or Si based electrical power devices. The deep traps and electronic disorder produced by light ion irradiation can modify the electrical, magnetic, and optical properties of films (e.g., dilute ferromagnetic semiconductors and topological materials). Additionally, benefiting from the high reproducibility, precise manipulation of functional depth and density of defects, as well as the flexible patterning ability, the helium or proton ion irradiation has been successfully employed in improving the dynamic performance of SiC and Si based PiN diode power devices by reducing their majority carrier lifetime, although the static performance is sacrificed due to deep level traps. Such a trade-off has been regarded as the key point to compromise the static and dynamic performances of power devices. As a result, herein the light ion irradiation is highlighted in both exploring new physics and optimizing the performance in functional materials and electrical devices.

Key words: ion irradiation; power device; crystal; thin film; functional materials

Citation: Y Yuan, S Q Zhou, and X Q Wang, Modulating properties by light ion irradiation: From novel functional materials to semiconductor power devices[J]. *J. Semicond.*, 2022, 43(6), 063101. <https://doi.org/10.1088/1674-4926/43/6/063101>

1. Introduction

Ion beams present a variety of useful functions in the field of semiconductors, acting as the state-of-the-art tools for both basic research and industry. In particular, it is worth noting that ion implantation has been integrated as one of the most crucial processes in modern IC industry^[1, 2]. Recently, a number of novel functional semiconductors have been successfully fabricated by ion implantation at high fluence and ultra-fast annealing^[3–10]. For such instances, the implantation is highlighted to overcome the obstacle of solubility limit of impurities in semiconductors, which is always treated as the main challenge of conventional equilibrium methods.

In addition to the above-mentioned well-known doping contributions introduced by implanted ions themselves, point defects are spontaneously produced in the semiconductor matrix due to the collisions between incident ions and the matrix atoms. The interaction between implanted ions and target atoms could be briefly described as follows: by undergoing collisions with the electron system and the nuclei of the target matrix, the impinged ions gradually lose the kinetic energy. At the very beginning, the kinetic energy loss is mainly caused by the electronic stopping (excitation and inelastic atom ionization), which dominates in the high energy regime. In such a regime, the implanted ions prefer a straight moving path, and the main stopping mechanism of interac-

tion mainly comes from the inelastic interactions between bound electrons in the matrix atoms and the implanted ions. Therefore, the inelastic interaction is highlighted to be responsible for the energy lost, accordingly, this part of transferred energy is partially dissipated by phonons; however, the displacement of lattice atoms seldomly happens. Afterwards, upon penetrating into deeper depth, the implanted ions start to confront nuclear stopping due to their low kinetic energy, in which the displacement of atoms starts to dominate and even leads to a cascade of recoiled atoms. This process is named nuclear stopping, which mainly refers to the elastic instead of inelastic collisions between the projectile ions and matrix atoms in the target. It is worth noting that the nuclear stopping means that this type of stopping involves the collision of the ion with the nuclei in the target. At this moment, the point defects start to accumulate. A schematic of relative loss of kinetic energy is shown in Fig. 1 to make a comparison between electronic and nuclear stopping processes with their dependence on ion kinetic energy^[11, 12]. This figure qualitatively shows that the ability of nuclear stopping is weaker than the electronic stopping process, and it mainly works when the ion energy is very low. The stopping power gradually decreases upon increasing ion energy, and the contribution disappears when the ion energy is high. However, the contribution from the electronic stopping process always exists, but plays mostly at the high ion energy part as a maximal peak.

The above-mentioned point defects can provide additional functionalities in semiconductor materials. In particular, light ions (e.g., proton, helium as well as some other ions whose atomic numbers are relatively small) are beneficial for a better access of thick films/devices, as well as for a

Correspondence to: Y Yuan, yuanye@sslab.org.cn; X Q Wang, wangshi@pku.edu.cn

Received 17 NOVEMBER 2021; Revised 5 MARCH 2022.

©2022 Chinese Institute of Electronics

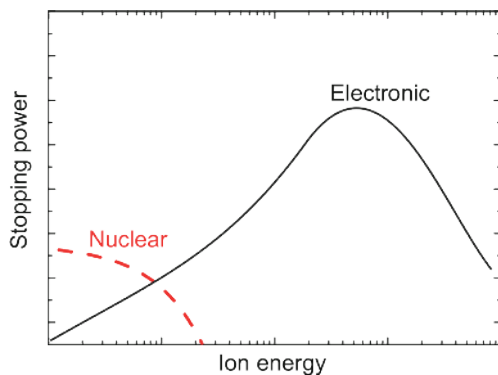


Fig. 1. (Color online) Schematic of the cross-section for electronic and nuclear stopping processes as a function of ion energy^[12].

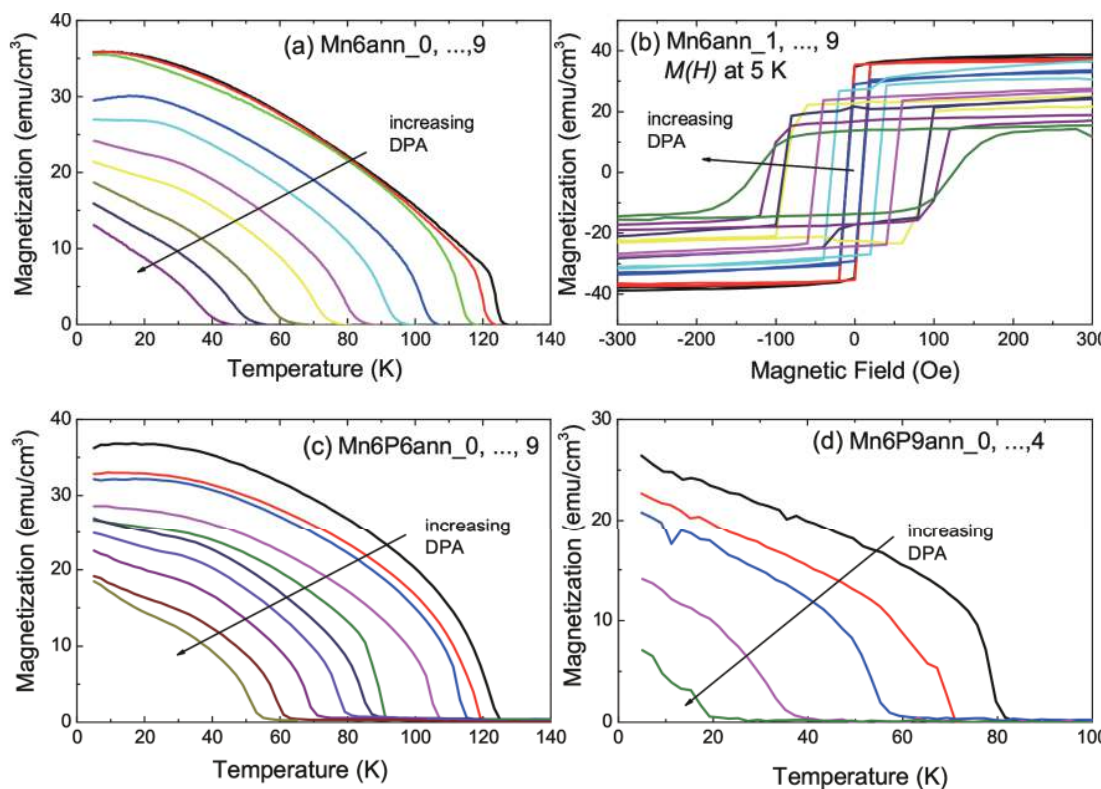


Fig. 2. (Color online) Magnetic properties after introducing hole compensation by ion irradiation. The ion fluence was increased in linear steps. (a), (c), and (d) show the temperature dependent magnetization for different samples, while (b) shows the magnetic hysteresis for sample Mn6ann (GaMnAs) for various ion fluences. The temperature-dependent magnetization is measured at a small field of 20 Oe after cooling in field. One observes an increase in the coercive field H_C when T_C and the remanent magnetization decrease. The arrows indicate the increase of DPA from 0 to 2.88×10^{-3} . In each panel, the black line is the result for the nonirradiated sample. This figure is drawn from Ref. [16].

radiation still has several merits, as follows: a) High throughput and reproducibility; b) Precise control of the density of generated defects and their depth profile by tuning the implantation fluence and energy; c) Flexible pattern for devices by combining conventional semiconductor industry techniques. For instance, by combining the photolithography and mask, the ultrahigh dense mid-submicrometre pixelation was achieved for augmented reality^[15].

In this short review, we will only focus on the application of light ion irradiation in tailoring the electronic properties of emerging functional materials^[16–19] and in modifying the dynamic performance of semiconductor power devices^[20, 21]. The other applications, such as doping semiconductors and “smart cut”^[22, 23], are not covered.

gentle control of the number of defects without inducing amorphization. Therefore, light ion irradiation is becoming more attractive in both condensed matter physics and semiconductor techniques. From the basic research viewpoint, the generated various vacancies or interstitials act as potential disorder, which in principle affects the electrical-transport properties (e.g., carrier mobility), and therefore highlights the contribution of Anderson localization^[13]. Meanwhile, the introduced defects cause new energy levels located in the bandgap, and contribute intensively to the transport behavior, mostly by tuning carrier concentration^[14]. Although several avenues have been explored to involve the point defects in functional material matrix (e.g., non-stoichiometric growth), it is worth mentioning that the light ion ir-

2. Manipulating defects in conventional and novel functional materials

2.1. Tuning the Fermi level in dilute ferromagnetic semiconductors

Dilute ferromagnetic semiconductors (DFSs) have been viewed as the one of the most fancy topics in the past several decades. Due to the nature of hole-mediated ferromagnetism in DFSs, any methods used in tuning carrier concentration^[24] (e.g., electrical gating or co-doping) can be used to modify ferromagnetic properties or explore the interplay between electrical and ferromagnetic features. Thus, as expected, the light ion irradiation just fulfills the requirement of carri-

er density modification^[16, 25] by compensating carriers through introducing deep level traps, afterwards creating a platform to understand the physics in DFSs.

Since the discovery of DFSs, the mechanism of hole-mediated ferromagnetism has always been placed at the center of the argument, where the competition between *p-d* Zener model and the impurity model never stops. In the *p-d* Zener model the randomly distributed Mn moments are bridged by the itinerant valence band holes^[24], while the localized holes in the isolated impurity band dominate the mediation according to the impurity band model^[26]. Expectedly, ion irradiation allows the flexible manipulation of carrier concentration, by which the Fermi level could be shifted in a large range from the valence band towards the bandgap. This helps a lot when exploring the interplay between carrier localization and magnetism in DFSs. Before the irradiation, H⁺ plasma is initially proposed to control ferromagnetism in DFSs by Goennenwein *et al.*^[27]: The H⁺ plasma successfully drives the GaMnAs from ferromagnetic state with ~70 K Curie temperature into paramagnetic state by compensating holes. Enlightened by the idea of H⁺ plasma, light ion irradiation was utilized to intentionally produce the tapping defects in GaMnAs, and magnetization and magneto-transport were both manipulated^[28]. In 2016, a more systematic picture in irradiated GaMnAs was depicted^[16]: By increasing fluences, irradiation results in a raised lattice disorder, quantified by displacement per atom (DPA), leading to an enhanced carrier compensation. As a result, the system changes from original metallic to insulating state, confirming the gradual departure of the Fermi level from valence band into the bandgap^[16]. For magnetic properties, it is observed that the saturation magnetization, remanent magnetization as well as Curie temperature decrease upon increasing DPA, which is in agreement with the description of *p-d* Zener model. As shown in Fig. 2, the temperature dependent magnetization of GaMnAs, GaMnAs_{0.94}P_{0.06} as well as GaMnAs_{0.91}P_{0.09} under different irradiation fluences is displayed: upon increasing the DPA by raising irradiation fluences, the temperature dependent magnetization curve gradually deviates from the mean-field theory described convex shape, which indicates that the system is away from the global ferromagnetism. It is worth noting that by benefiting from carefully tuning irradiation fluence, it is possible to capture detailed statues of the whole evolution process, which further helps when analyzing the correspondence between carrier localization and magnetization reduction. As a result of the irradiation induced hole-compensation, the Fermi level shifts back to the bandgap, while magnetism is gradually deviated from the global ferromagnetism due to the weakened hole mediation. Consequently, the nano-scaled electronic phase separation appears and the long-range ferromagnetic coupling is interrupted. In addition to the reduced magnetism, it has been also verified that the uniaxial magnetic anisotropy is manipulated by irradiation, through shifting the Fermi level between the splitting valence band^[25]. The successful anisotropy modification again confirms the validation of *p-d* Zener model.

Besides the most widely studied GaAs based DFSs, the proton irradiation can also stabilize the Fermi level in relatively different positions in the bandgap in various III-V matrixes^[29]. Therefore, it is easy to imagine that the same irradiation condition would perform different compensation effects in various matrixes, further contributing discriminately to the magnet-

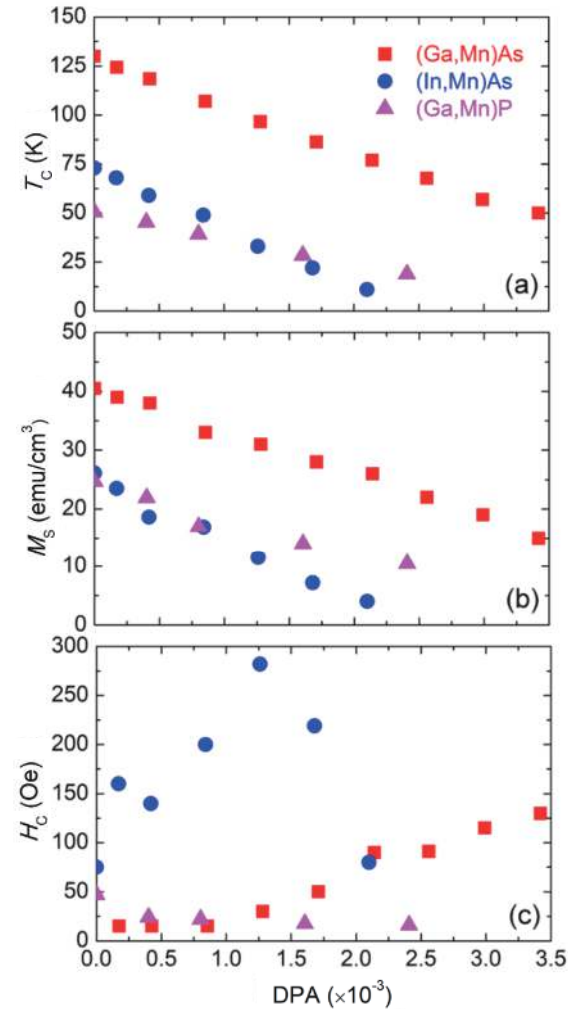


Fig. 3. (Color online) (a) Curie temperature (T_c), (b) saturation magnetization (M_s) as well as (c) coercive field (H_c) for the magnetic easy axis at 5 K versus DPA for (Ga,Mn)As (squares), (In,Mn)As (circles) and (Ga,Mn)P (triangles)^[17].

ism manipulation. As expected, the above-mentioned deduction was confirmed by our previous work that the same DPA results in the different magnetism-modification in GaMnAs, InMnAs and GaMnP. As shown in Fig. 3, the DPA dependent saturation magnetism and T_c curves show different slopes, which unambiguously confirms that the produced defects work differently in different III-Mn-V compounds.

In addition to the dilute magnetic semiconductors whose properties are strongly coupled by carriers, plenty of novel proposed functional materials also require such a method of carrier-modulation. In particular, the recently exotic topological properties in various topological materials are also reflected through electrical carriers; therefore, the ion irradiation would definitely be an ideal tool for investigation.

2.2. Generating potential disorder in topological materials

In addition to modifying the Fermi level by introducing carrier compensation, in some cases, the structural or potential disorders caused by irradiation induced defects can significantly influence electrical-transport properties, even though the carrier concentration remains constant^[30]. With the presence of disorder, the mean free path is disturbed due to the break of long-range Bloch extended potential, and con-

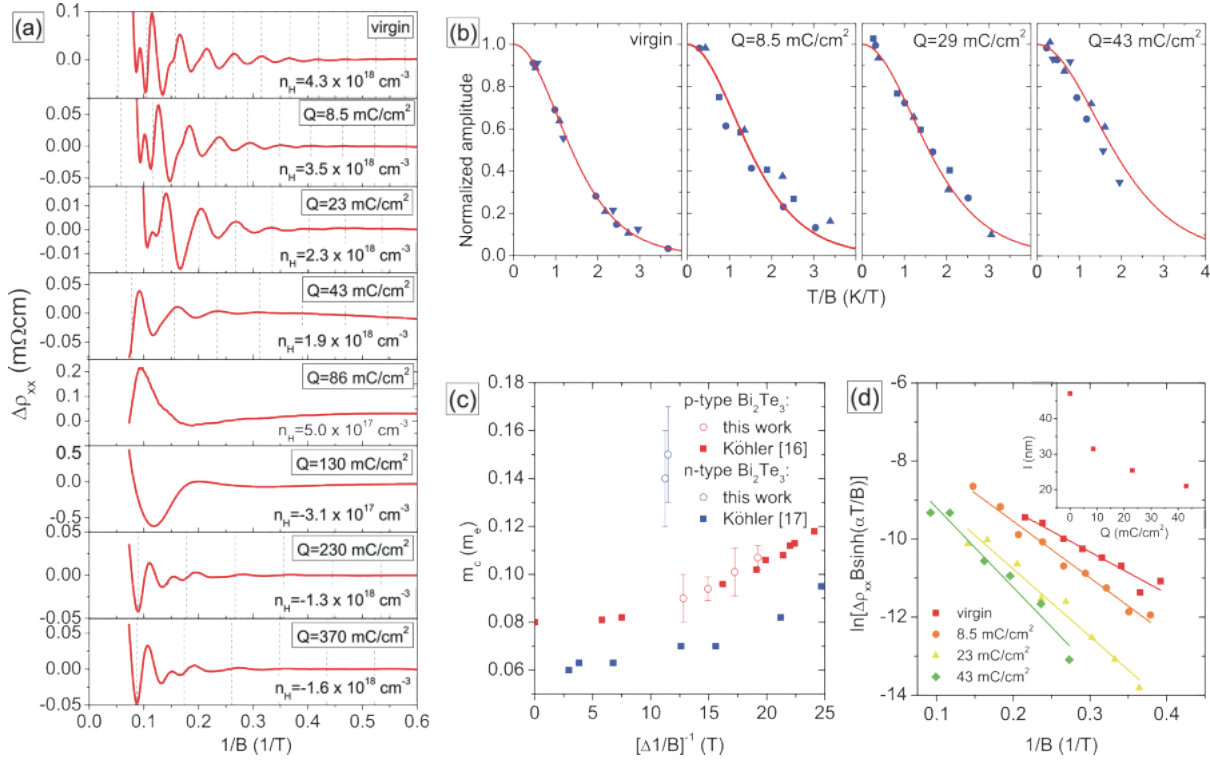


Fig. 4. (Color online) (a) Oscillating part of the resistivity $\Delta\rho_{xx}$ at 1.9 K for $B \parallel c$ as a function of the inverse magnetic field $1/B$ for different irradiation doses. (b) Temperature dependence of the oscillation amplitude with solid lines representing the fits obtained using the equation of Eq. (2). Different symbols correspond to the analysis of different Landau levels (i.e., peaks at different $1/B$ positions). To compare the temperature dependence of different peaks, the oscillation amplitudes have been normalized to the value of the fit for $1/B \rightarrow 0$. (c) Cyclotron masses m_c as function of the inverse oscillation period $[\Delta(1/B)]^{-1}$. (d) Dingle plots at $T = 1.9$ K and inset showing the mean free path l as a function of irradiation dose Q ^[18].

sequently the effect of Anderson localization is largely enhanced and carriers become more localized^[31]. In some systems, both the carrier compensation and potential disorder cooperatively change magneto-transport properties. Thus, ion irradiation can be employed as a useful tool to investigate the above mentioned two contributions, particularly in recent topological insulators/superconductors^[18, 32, 33].

By borrowing the concept of Fermi level tuning in DFSs, the validity of manipulating carrier type or concentration through irradiation in a canonical topological insulator Bi₂Te₃ has been tested^[18]. Upon increasing electron irradiation fluences, the up-shift of the Fermi level is clearly observed together with a turnover of conductivity from p to n type. The detailed evolution of the electrical transport behavior can be explored by Shubnikov-de-Haas (SdH) oscillation which is popular in systems with high carrier mobility. With increasing magnetic field, the movement of spin-split Landau levels causes the periodical oscillation of resistance, including both longitudinal resistance (ρ_{xx}) and Hall resistance (ρ_{xy}). By carefully analyzing the period and magnitude of the oscillation through fast Fourier transformation, it is possible to obtain the effective mass, the carrier density, as well as the mean free patch according to the standard Lifshitz-Kosevich theory^[34]. The SdH period $\Delta(1/B)$ is expressed as Eq. (1):

$$\Delta\left(\frac{1}{B}\right) = \frac{2\pi e}{\hbar S_F} = \frac{e\hbar}{m_c \epsilon_F}, \quad (1)$$

S_F is the cross section of the Fermi surface perpendicular to

the direction of the field B , m_c is the cyclotron mass, \hbar is the Planck constant, and ϵ_F is the Fermi energy (measured from the band edge). The standard Lifshitz-Kosevich theory is described as Eq. (2):

$$\Delta\rho_{xx}\left(\frac{T}{B}\right) = \frac{aT}{B \sinh(aT/B)}, \quad (2)$$

where $a = \frac{2\pi^2 m_c k_B}{\hbar e}$. This equation allows for the extraction of m_c . As shown in Fig. 4(a), with the dependence of irradiation fluences from 8.5 to 370 mC/cm², the oscillation of $\Delta\rho_{xx}$ (obtained by subtracting the background magnetoresistance) is tuned and accordingly the carrier concentration changes from 4.3×10^{18} (hole) to -1.6×10^{18} cm⁻³ (electron), presenting the donor characteristic of electron irradiation induced defects which are computationally assumed as Te vacancy clusters and Te_{Bi} antisite defects^[35, 36]. It is worth noting that the donor-like defects are produced not only by electron irradiation but similar phenomenon has also been observed in proton irradiated Bi₂Te₃ as early as in 1966, although at that time the Te interstitial was deduced as the origin^[37] and subsequently observed by transmission electron microscopy^[38]. However, there is a strong distinction of the m_c values from samples irradiated to 230 and 370 mC/cm². Moreover, as describing by the Dingle plot, the field dependent oscillation amplitude could determine the Dingle scattering time τ_D by plotting $\ln[\Delta\rho_{xx} B \sinh(aT/B)] \propto \pi m_c / (\epsilon_F \tau_D B)$ versus $1/B$ under determined T , as shown in Fig. 4(d). The mean free path l is described as Eq. (3) and such a value is also modified upon in-

creasing the irradiation fluence Q .

$$l = v_F T_D, \quad (3)$$

where the v_F is the Fermi velocity which is calculated by considering Eq. (1) and $\epsilon_F = \frac{mc_F^2}{2}$. As shown in Fig. 4(d), the mean free path l is also modulated by light ion irradiation. It can be concluded that the modification of carrier concentration by ion irradiation works not only in semiconductors, but also in high mobility topological materials, which expands the application matrix of ion irradiation.

Following the above discussion, the irradiation induced defects not only compensate carriers, but also produce electrical disorder which violates the highly ordered Bloch potential. It is well-known that in a material with low mobility, the contribution of compensation is mainly in charge; however, in a high mobility system, the disorder effect starts to dominate. As described in Fig. 4(d), the mean free path reduces in half and saturates when the fluence is 43 mC/cm^2 , which is indicative that the contribution of electrical disorder is comparable with that from the Fermi energy shift. Subsequently, such a disorder is treated as a meaningful tool to investigate the disorder contribution in other topological materials, such as $\text{Nb}_x\text{Bi}_2\text{Se}_3$ ^[39] and $\text{Sn}_{1-x}\text{In}_x\text{Te}$ ^[32]. For instance, according to the study by Smylie *et al.*^[39], due to the symmetry-protection, the superconducting state in doped topological NbBi_2Se_3 surprisingly presents its robust resistance to disorder-induced electron scattering, which is introduced by irradiation. As shown in Fig. 5, although the superconducting transition temperature T_C is gradually suppressed upon raising proton-irradiation fluences, both pristine and irradiated samples show quadratic dependence of London penetration depth versus temperature. This always happens in a clean system with linear quasi-particle dispersion around the point nodes in the superconducting gap^[39]. This result suggests that all samples are naturally clean, even though they have been irradiated under a variety of fluences. This is indicative of the appearance of the symmetry protected point nodes in $\text{Nb}_x\text{Bi}_2\text{Se}_3$. With the aid of irradiation, such an unexpected phenomenon was first seen and demonstrated the robustness of unconventional superconductor against the non-magnetic disorder, which means that the topological superconducting can be achieved in rather dirty systems.

According to this description, the ion irradiation is useful in modifying physical properties, which is related in carrier density in various functional materials. This carrier compensation contribution is strongly expected in application, due to its flexibility and manipulability. Therefore, in the next section, the employment of compensation caused by irradiation will be reviewed in improving the performance of electrical and electronic devices.

3. Manipulating the dynamic properties in semiconductor power devices

The explosion of electric power employment, particularly the preliminary success of electric-vehicles, is raising the unprecedented demand for p-n diode power devices. The switching speed (in particular switch-off) of these devices is becoming crucial for evaluating the comprehensive performance, particularly in high-frequency applications. The switch-off process can be described as follows: when the opposite

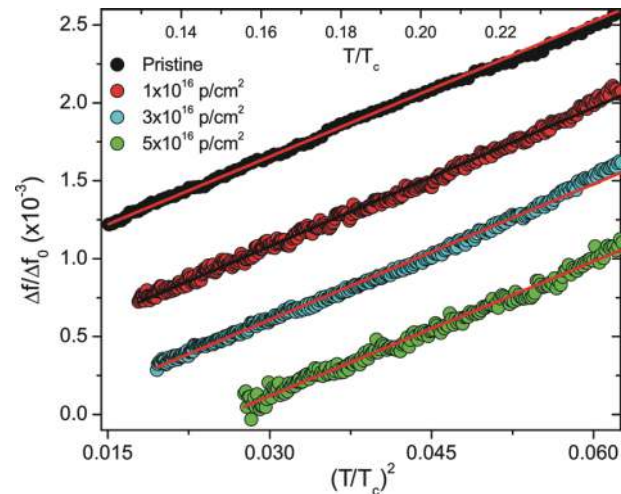


Fig. 5. (Color online) Low-temperature variation of the London penetration depth $\Delta\lambda(T)$ in a single crystal of $\text{Nb}_x\text{Bi}_2\text{Se}_3$ for multiple values of cumulative irradiation dose vs reduced temperature squared $(T/T_c)^2$. The linear fits (red, black lines) indicate quadratic behavior. As the dose increases, the temperature dependence remains quadratic, indicative of point nodes in the superconducting gap. Data are offset vertically for clarity of presentation. The top axis shows the corresponding T/T_c values^[39].

voltage is applied in the p-n diode, current flows through the diode in the opposite direction and spends some time to arrive at the stable state. During this process, the free minority carriers are first neutralized in both p and n regions and subsequently the carriers start to move and construct the depletion region. Accordingly, the whole period is called reverse recovery time and decides the switch-off speed. The expectation of improving dynamic performance starts the employment of light ion irradiation technique to tune the lifetime of the carriers. Although some conventional approaches such as diffusion life-killers have been maturely used in Si-based power devices, some shortages (e.g., short diffusion length or low sensitivity) still prohibit their utility in SiC-based devices^[40]. Additionally, by carefully playing the irradiation energy combined with photolithography, the ion irradiation allows precise and flexible modulation of carrier recombination in both in-plane and depth profile at micro- or nano-scale. However, the speed up of the device achieved by this approach is always accompanied with the sacrifice of blocking voltage, carrier mobility, and some other on-state static performance due to introduced defects (e.g., increasing the leakage and forward voltage)^[21, 41, 42]. Unfortunately, this modulation is treated as a trade-off between static and dynamic prerequisites. Nevertheless, part of irradiation caused defects can still be cured by thermo-treatments, which will partly recall the device status before the irradiation^[43]. As a result, the competition playground of irradiation vs. thermo-treatment works flexibly to track the optimal device performance. As discussed in former sections, various types of defects appear in the irradiated Si and SiC matrix, whose influence on the device performance varies, which will be mainly discussed in the next sections.

3.1. SiC semiconductor and SiC power device

Distinctive sets of defects in SiC are produced by irradiation, and the deep level transient spectrum (DLTS) is often

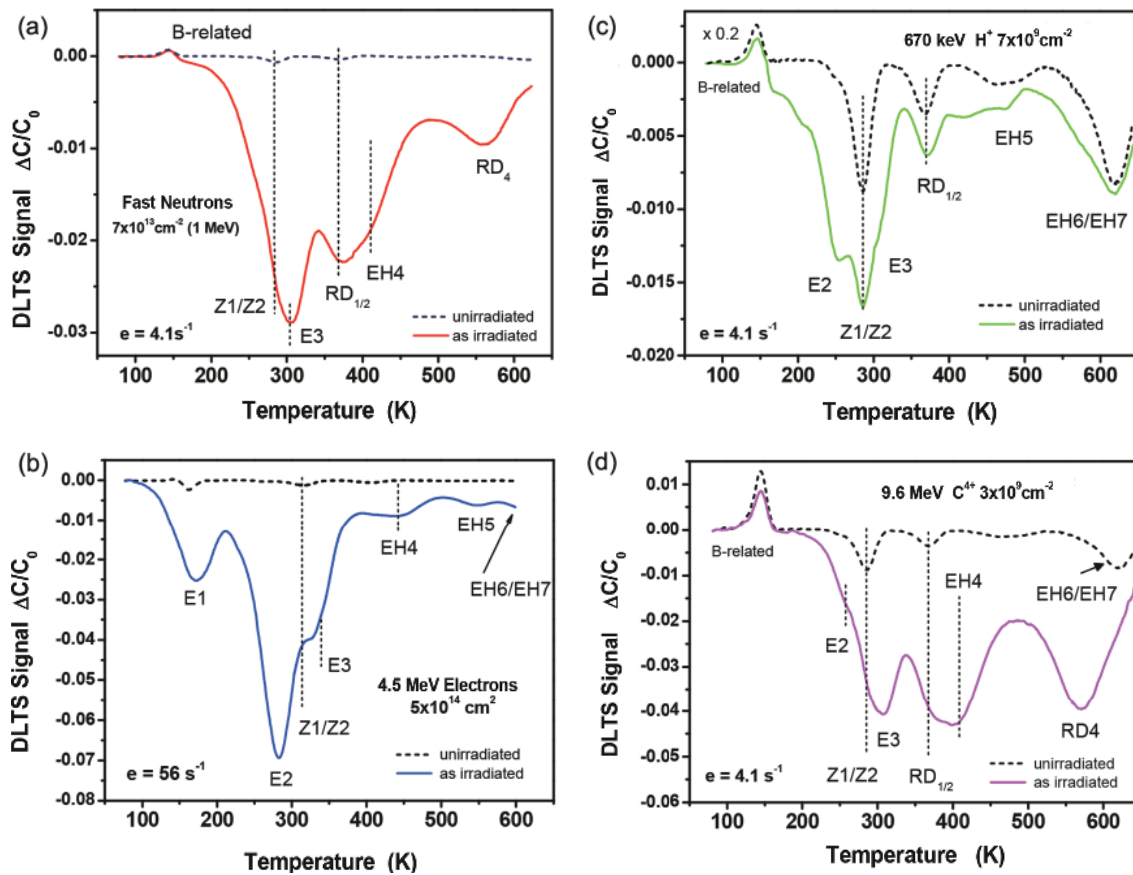


Fig. 6. (Color online) DLTS spectra of 4H-SiC n-type epilayer irradiated with (a) fast neutrons, (b) 4.5 MeV electrons, (c) 670 keV protons, and (d) 9.6 MeV carbon ions. First temperature scan, rate window 4.1 s^{-1} (neutron, proton and carbon irradiation) and 56 s^{-1} (electrons) [44].

employed to identify deep level defects. As shown in Fig. 6, Hazdra *et al.*'s results are present in fast neutrons, electrons, protons as well as carbon ions irradiated n-type 4H-SiC [44], and different deep traps are introduced in the bandgap. As shown in Fig. 6, the E₃ and E₂ deep levels are mainly caused by fast neutrons (1 MeV, $7 \times 10^{13}\text{ cm}^{-2}$), carbon ions (9.6 MeV, $3 \times 10^9\text{ cm}^{-2}$) as well as electrons (4.5 MeV, $5 \times 10^{14}\text{ cm}^{-2}$), while the Z_{1/2} trappers are caused by proton irradiation (670 keV, $7 \times 10^9\text{ cm}^{-2}$). The origin of this distinction is the different collision effect between the implanted ions and the host matrix, which comes from the different nuclear stopping ability of elemental atoms in various semiconductors [11]. As a result, various defect complexes that consist of various elemental vacancies appear in the material [45, 46], and accordingly the induced traps are located in different levels in the bandgap [47, 48]. Most of them work as carrier trap centers in the matrix and reduce the lifetime of carriers, whereas only the thermo-stable ones are preferential when being considered functionally and stably in device. Many researchers have focused on the thermo-behavior of various traps, and finally the Z_{1/2} is successfully qualified because of its persistence at temperatures even above 2000 °C [49–51]. Additionally, the advantage as a prominent lifetime monitor also places Z_{1/2} in the center of the lifetime engineering stage [52]. From the fundamental research point of view, plenty of efforts have been made to clarify the birth of Z_{1/2} defects and various hypothesizes have been proposed. In the very early stage, the Z_{1/2} defects were found in nitrogen doped SiC, and the correlation between the trap density and N dopant was de-

duced [53]. Accordingly the most proper candidate model of Z_{1/2} trap was formulated as the configuration of an nitrogen atom neighboring with dicarbon interstitials [54]. However, the subsequent experiment ruled out such an assumption in terms of observing the dependence of Z_{1/2} concentration in P doped SiC when the density of doping phosphorus is almost one magnitude higher than that of nitrogen. Interestingly, this experiment excluded the possible participation of nitrogen in the complex [55]. According to subsequent studies, it is found that the Z_{1/2} defect is a kind of intrinsic defect complex in the SiC matrix and it is caused by two possible configurations: (i) silicon vacancy combined with carbon interstitial (Si_v+C_{int}) or (ii) carbon vacancy neighbored with silicon interstitial (C_v+Si_{int}). Experimental results increasingly favor the latter model, such as by carbon implantation [56] or annealing of electron irradiated SiC. Even though a lot of attentions have been paid to this topic, the clarification of the Z_{1/2} defect is still limited. Nevertheless, this does not shake its role as carrier life-time manipulator in SiC devices.

To modulate the carrier lifetime, several approaches have been employed to demonstrate or excavate the function of Z_{1/2} before the light ion irradiation technique is imported: the annihilation of Z_{1/2} defects extends the carrier lifetime. For instance, several studies have shown that the carrier lifetime in carbon-implanted SiC is increased by high temperature annealing [56, 57]. The lifetime was also pronouncedly enhanced in as-grown SiC layers by high temperature annealing [50]. In addition, another alternative method to promote the lifetime through killing Z_{1/2} is the thermo-oxidation. For example, ac-

Table 1. Parameters for proton irradiation induced deep levels in n-type SiC.

Level	Energy (eV)	Ref.
T ₁	$E_C - 0.17$	[20, 60]
EH ₁	$E_C - 0.42$	[20, 59, 61, 62]
Z _{1/2}	$E_C - 0.66$	[20, 43, 50, 57, 59, 63]
EH ₃	$E_C - 0.72$	[20, 44, 59, 62]
EH ₅	$E_C - 0.80$	[49]
T ₂	$E_C - 1.41$	[60]
EH _{6/7}	$E_C - 1.64$	[49, 64]

cording to studies from Kimoto, through eliminating the Z_{1/2} density, carrier lifetimes were prolonged from 1.1 and 0.73 μ s to 33.2 and 1.62 μ s, respectively, by thermo-oxidation [43, 58]. In contrast, it is also meaningful to intentionally build up Z_{1/2} defects in some cases where a short lifetime is required (e.g., high frequency p-n junction). As shown in Fig. 6, the proton irradiation (sometimes electron irradiation) that is an effective way for producing Z_{1/2} is strongly recommended. Actually, a series of defects are produced by proton irradiation together with Z_{1/2} trap, as displayed in Table 1. However, mainly the Z_{1/2} and EH_{6/7} can survive after the subsequent low temperature annealing and they improve the performance of p-n junction SiC device [20, 59]. As shown in Fig. 7, several signals at around 300, 440, 570 and 660 K appear in irradiated samples but are absent in the as-grown one, confirming the vacancy-production via proton irradiation. Although the subsequent annealing cures the defects of EH₁ and EH₃, intensive Z_{1/2} and EH_{6/7} peaks still can be observed at around 300 and 660 K, which definitely verifies their thermo-stabilization, and thus determines their qualification as lifetime tailors.

Z_{1/2} locates at about 0.44 eV below the bottom of the conduction band, acting as the main local lifetime killer in terms of its large capture cross section for both electrons and holes. When Z_{1/2} centers are placed in the n-region of p-n diode junction, the electrons (majority carriers) are strongly compensated in the defect-profiled space, therefore speeding up the device turn-off process. On the basis of the study from Hazdra *et al.* [20, 59], the proton irradiated 10 kV/2 A PiN diode SiC chip under fluence of $1 \times 10^{11} \text{ cm}^2$ at an 800 keV energy presents 2.5 times reduction of reverse recovery charge when compared with the unirradiated one. As shown in Fig. 8, it is seen that the maximum of the reverse recovery current cuts in half accompanied with a faster and softer switch-off, even though the subsequent annealing partly compensates the irradiation contribution. In addition to reverse recovery waveforms, the open circuit voltage decay (OCVD) is also employed to evaluate the high-level lifetime (τ_{HL}) that is calculated from the slope of dV/dt response, which manipulates the time dependent term of the post injection voltage [65]. As shown in Fig. 9, the irradiated device exhibits a larger slope in the quite initial recovery part, while it negligibly contributes to the slope of the rest part. According to the inset of Fig. 9, upon increasing the irradiation fluences to $1 \times 10^{10} \text{ cm}^{-2}$, the τ_{HL} is successfully tuned from around 2.8 μ s down to around 1.6 μ s, but it saturates when the fluence continues to increase. Note that to achieve such fast switch-off, it is necessary to place the defected region at the anode side of the n-base in the PiN structure, which is similar as in silicon-based p-n junction and will be reviewed in the next section.

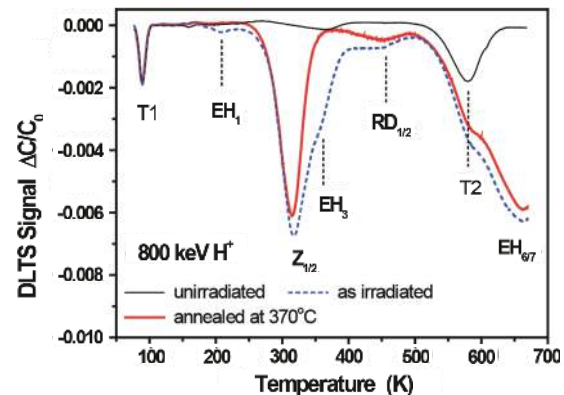


Fig. 7. (Color online) DLTS spectra of n-base of the 4H-SiC PiN diode measured before (black thin) and after (short-dashed) irradiation with 800 keV protons to a fluence of $5 \times 10^9 \text{ cm}^{-2}$ and after annealing at 370 °C [59].

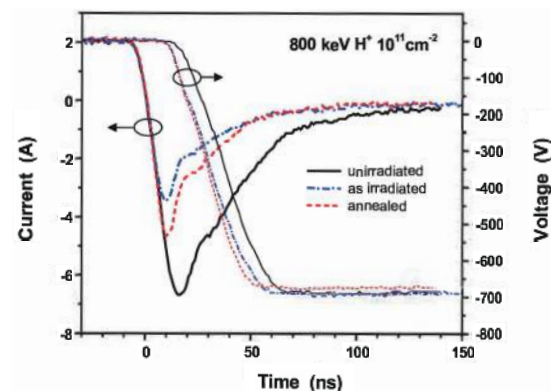


Fig. 8. (Color online) Reverse recovery of the 2 A/10 keV SiC PiN diode measured before (solid line) and after irradiation (dashed-dotted line) with 800 keV protons to a fluence of $1 \times 10^{11} \text{ cm}^{-1}$ and after subsequent 1 h annealing at 370 °C [20].

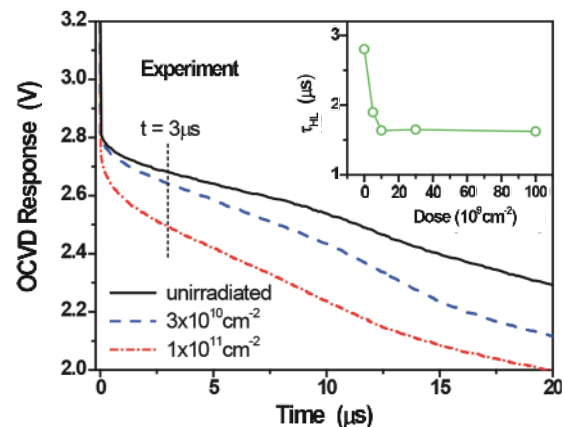


Fig. 9. (Color online) Measured OCVD response of 4H-SiC PiN diodes irradiated with different fluences of 800 keV protons. The value of high-level lifetime τ_{HL} (extracted at $t = 3 \mu\text{s}$) for different irradiation fluences is shown in the inset [59].

In addition to the most wanted Z_{1/2}-type defect, the SiC based p-n device is unavoidably affected by other various type defects, of which the most crucial one is EH_{6/7}, whose thermo-stabilization is at the same level as Z_{1/2}. EH_{6/7} lies 1.64 eV below the bottom of conduction band (even in the center of the bandgap), which is much deeper than Z_{1/2}. As a con-

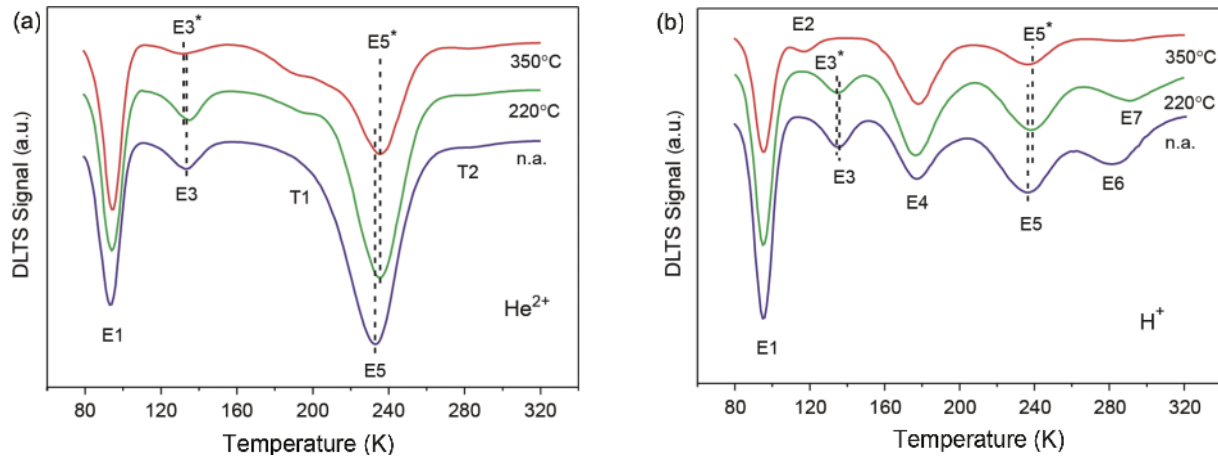


Fig. 10. (Color online) Majority carrier DLTS spectra of P⁺PN-N⁺ diode measured after (a) He⁺ irradiation and (b) H⁺ and isochronal 40 min annealing at 220 and 350 °C, rate window 260 s⁻¹ [69].

Table 2. Survey of deep level electron traps identified in proton and He irradiated silicon [69, 72].

Level	Bandgap position (eV)	Capture cross section (cm ²)	Identity
E ₁	$E_C - 0.167$	$\sigma_n = 4 \times 10^{-15}$	VO ^(-/-) +C _i -C _s ^(-/-)
E ₂	$E_C - 0.213$	$\sigma_n = 1 \times 10^{-14}$? (H-related)
E ₃	$E_C - 0.252$	$\sigma_n = 7 \times 10^{-15}$	V ₂ ^{=/-}
E ₄	$E_C - 0.312$	$\sigma_n = 4 \times 10^{-15}$	VO-H
E ₅	$E_C - 0.436$	$\sigma_n = 3 \times 10^{-15}$	V ₂ ^{-/0}
E ₆	$E_C - 0.463$	$\sigma_n = 2 \times 10^{-16}$	H-related (V ₂ H)
E ₇	$E_C - 0.507$	$\sigma_n = 6 \times 10^{-17}$? (H-related)

sequence, they work as charge producer in the space charge region, leading to the diode leakage (off state losses) in irradiated devices. Another negative effect brought by deep level traps is the increase of the forward voltage drop due to the compensation induced electron reduction, which has been observed in a set of various SiC based devices, e.g. PiN diode [20], MPS power diode [21] as well as JBS diode [42, 44]. In summary, when the proton irradiation is employed, it is necessary to trade off the balance between dynamic and static performance according to the requirement.

3.2. Si semiconductor and Si power device

Despite the fact that many alternative candidates (e.g., SiC or GaN) have been attracting attention, silicon still occupies the main part of power device market due to its mature industrial process. Thus, it is meaningful to review the manipulation of silicon as well as the corresponding device modified by light ion irradiation. Indeed, the irradiation contribution to silicon devices initiated the followed-up activities in SiC diodes, including IGBTs [66], PiN diode power device [67–69], as well as power thyristors [70, 71]; tuning the lifetime of majority carriers through producing deep level traps. According to studies in the past several decades, irradiation induced defects in silicon have been fully explored, such as E₁, E₂, E₃, E₄, E₅, E₆ as well as E₇, and detailed information is displayed in Table 2. As discussed in former sections, the capture cross section and thermo-stability are both treated as key criteria to evaluate the ability as lifetime-modulator. Overall, two types of defects that, respectively, locate 0.167 eV (from vacancy-oxygen pair VO^{-/0}, defined as E₁) and 0.436 eV (from divacancy

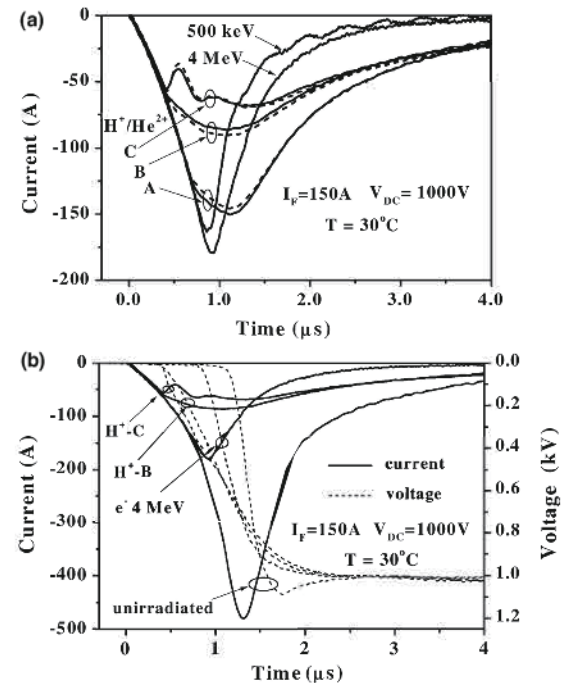


Fig. 11. (a) Current reverse recovery characteristics of diodes irradiated by 500 keV ($3 \times 10^{14} \text{ cm}^{-2}$) and 4 MeV ($2 \times 10^{13} \text{ cm}^{-2}$) electrons (solid thin) and H⁺/He²⁺ ions (fluence $5 \times 10^{12} / 5 \times 10^{11} \text{ cm}^{-2}$, thick solid/dashed); (b) current (solid) and voltage (dashed) reverse recovery characteristics of the unirradiated diode and diodes irradiated by 4 MeV ($2 \times 10^{13} \text{ cm}^{-2}$) electrons and H⁺ ions (fluence $5 \times 10^{12} \text{ cm}^{-2}$) [73].

V₂^{-/0}, defined as E₅) below the bottom of conduction band are most important for tuning carrier lifetime. As shown in Fig. 10, the lighter proton contributes less E₅ defects when compared with the He irradiation. This phenomenon is explained by the fact that the light projectiles (e.g., protons or electrons) produce fewer complex defects (e.g., interstitials and vacancies), which subsequently neighbor with impurities and form vacancy-impurity complexes. Meanwhile, the divacancies are more probable to give birth under heavy ion irradiation [69]. Moreover, as shown in Fig. 10, E₁ and E₅ both exhibit pronounced thermo-stability, presenting their possible use as majority carrier life-time manipulators.

The exploration of tuning life-time in silicon p-n type

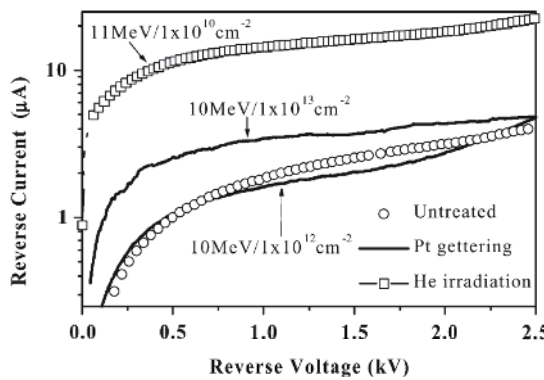


Fig. 12. The reverse I - V curves measured at 30 °C of the unirradiated and not annealed device (Untreated), the irradiated double Al electrode devices with He energy of 11 MeV and dose of $1 \times 10^{10} \text{ cm}^{-2}$ (He irradiation), and the PtSi + Al electrode devices with He energy of 10 MeV and doses of 1×10^{12} and $1 \times 10^{13} \text{ cm}^{-2}$, both annealed at 700 °C for 20 min (Pt gettering)^[76].

device has been performed in the past decades. As shown in Fig. 11, when the irradiation project range is placed in different depth (e.g., the anode side of the junction inside (outside) of the space charge region) and the N base side of the junction, their distinct contribution works on the lifetime of the p-n device^[73]. Due to the nature of produced electron traps, it is expected that an optimal manipulation would happen when the projects range locates in the N base. This expectation was subsequently verified in many studies. As shown in Fig. 11, with both irradiation with proton and alpha particles, the measured reverse recovery waveforms of irradiated devices indicate that the sloping lifetime is obviously reduced by irradiation and furthermore results in the speed-up of the switch-off process^[67, 69, 72, 73].

The trade-off that happens in SiC devices is also inevitable in Si: the fast switch-off process is always accompanied with the sacrifice of forward voltage and current leakage. Of all generated defects, E₅ is always treated as the charging role who is responsible for the leakage, which is attributed to its location in the middle of the bandgap^[74]. As a result, the irradiation with lighter ions (e.g., protons or electrons) is preferred due to the less presence of E₅ defects to balance the trade-off between the dynamic benefit and static sacrifice. Afterwards, solving this challenge by modifying the other function part in the device (e.g., a novel electrode) was explored^[75–77]. The aim is to improve the ohmic contact by using a very low resistance electrode at the anode, which can partly compensate the sacrificed static characteristics induced by irradiation. According to studies from Vobecky *et al.*, replacing the conventional aluminum or Ti-Ni-Ag electrode by platinum-silicide compound at the anode region outstandingly improves the drawback of raised leakage current and forward voltage. Actually, such a PtSi electrical contact could be achieved in a number of ways, such as the conventional platinum diffusion^[78] or the proximity gettering^[79]. As shown in Fig. 12, it is easy to note that according to the comparison between devices with PtSi+Al and Al+Al electrodes, the leakage current of device involved with PtSi contact was largely suppressed, which is even comparable with the value of un-irradiated device. Most importantly, the charge carrier life-time remains constant, which means that the novel electrode does not negatively affect the dynamic properties. In ad-

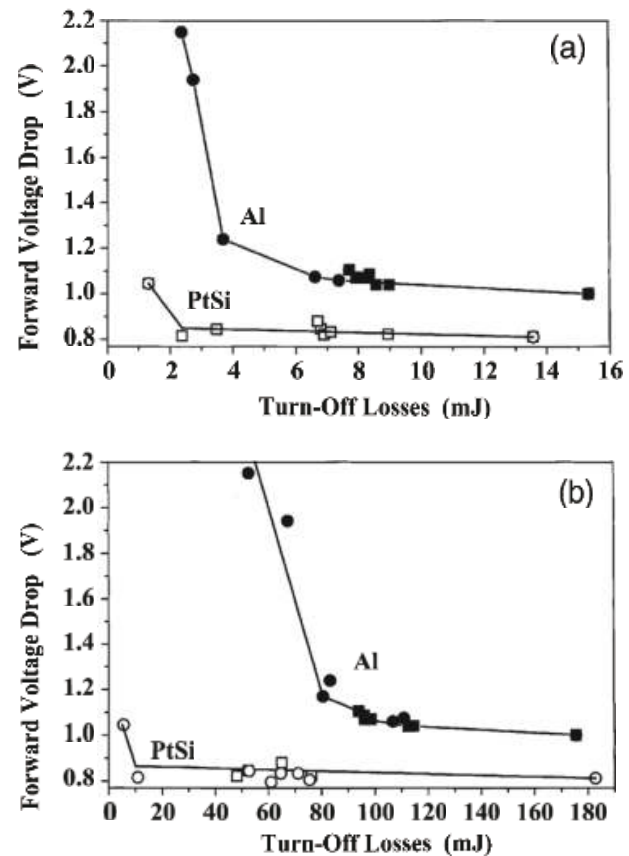


Fig. 13. Trade-off between the ON-state voltage drop at 100 A and the turn-OFF losses measured at (a) $V_{DC} = 500 \text{ V}$, $J_f = 1 \text{ A/cm}^2$ and (b) $J_f = 50 \text{ A/cm}^2$ for unirradiated and helium irradiated devices whose electrodes are PtSi and Al. The irradiation energies are 5.8 MeV (open squares) and 10 MeV (open circles) for the sample with PtSi anode and 7.1 MeV (solid squares) and 11 MeV (solid circles) for the sample with Al anode^[75].

dition to the reverse current, the drop of the forward voltage is also partly cured by the involvement of PtSi anode electrode. As displayed in Fig. 13, this trade-off phenomenon is nicely elaborated by forward voltage drop versus turn-off losses in both low (1 A/cm^2) and high (50 A/cm^2) current density cases: upon increasing the irradiation energy, the turn-off loss reduces meanwhile the forward voltage drop increases. However, it is worth noting that by employing the PtSi anode, the drop of voltage remains constant, although the turn-off loss decreases till 2.2 and 10 mJ under the current densities of 1 and 50 A/cm^2 , respectively. For the double Al anode samples, the voltages start to dramatically raise at 4 and 80 mJ which are two and eight times higher than the values of PtSi anode-equipped sample. By considering the absolute value of voltage drop, the compound anode also shows outstanding performance, in which the PtSi device irradiated under highest fluence presents similar voltage drop level (around 1.1 V in both low and high current density cases) as in unirradiated devices using Al electrodes, as shown in Fig. 13. Therefore, it can be concluded that the employment of such novel anode would improve the static performance in SiC based devices.

Finally, it is worth noting that herein we only reviewed the application of ion beams in two types of functional materials and semiconductor devices. The ion beam only provides an avenue for modifying Fermi level in materials, and it could

be expanded in any other materials. It could be utilized as long as various new functional materials are developed; for example the ion beam modification is recently employed in very hot 2D materials^[80, 81] and semiconductor quantum computation fields^[82–84]. In particular, for some novel semiconductors or corresponding p-n devices (e.g., Ga₂O₃ which recently became attractive because of its ultra-wide bandgap characteristic)^[85–88] the ultra-high bandgap allows for huge sacrifice space for static performance. Therefore, it leaves lots of potential to improve the dynamic performance by irradiation. Consequently, material modification by ion beams in more novel functional materials can be expected.

4. Summary

In summary, the application of light ion (proton or alpha particle) or electron irradiation in modulating the properties of both novel functional materials and PIN power devices has been systematic reviewed. By properly employing the irradiation-induced defects, which generally act as carrier traps, it is possible to precisely tune the carrier concentration. This compensation can be used to study/tune some properties that are determined by the carrier concentration (e.g., the Curie temperature, magnetization as well as uniaxial magnetic anisotropy in dilute ferromagnetic semiconductors or electrical-transport properties in topological materials). The compensation reduces the carrier's life-time, which directly contributes to improving the dynamic performance of Si or SiC based PiN power devices, although several static performance parameters, including the forward voltage and current leakage, are somehow sacrificed. Nevertheless, this trade-off has been well played to fulfill different application requirements. Considering the explosion of novel functional materials and the energy revolution, it is believed that the light ion irradiation technique will find favor in both fundamental research and industrial applications.

Acknowledgements

This work was supported by Key-Area Research and Development Program of Guangdong Province (No. 2019B010132001). This work was also partially funded by Guangdong Basic and Applied Basic Research Foundation (2020A1515110891).

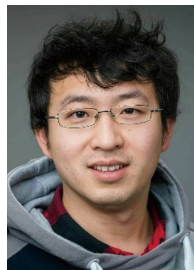
References

- [1] Mayer J, Marsh O. Ion implantation in semiconductors. *Appl Solid State Sci*, 1969, 1, 239
- [2] Stephen J, Dearnaley G, Freeman J H, et al. Ion implantation. Book Review, 1973
- [3] Yuan Y, Xu C, Hubner R, et al. Interplay between localization and magnetism in (Ga, Mn)As and (In, Mn)As. *Phys Rev Mater*, 2017, 1, 054401
- [4] Yuan Y, Wang Y, Khalid M, et al. Ferromagnetic GaMnP prepared by ion implantation and pulsed laser annealing. *IEEE Trans Mag*, 2014, 50, 2401304
- [5] Yuan Y, Wang M, Xu C, et al. Electronic phase separation in insulating (Ga, Mn)As with low compensation: Super-paramagnetism and hopping conduction. *J Phys Condens Matter*, 2018, 30, 095801
- [6] Yuan Y, Hubner R, Liu F, et al. Ferromagnetic Mn-implanted GaP: Microstructures vs magnetic properties. *ACS Appl Mater & Interfaces*, 2016, 8, 3912
- [7] Yuan Y, Wang Y, Gao K, et al. High Curie temperature and perpendicular magnetic anisotropy in homoepitaxial InMnAs films. *J Phys D*, 2015, 48, 235002
- [8] Prucnal S, Heera V, Hübner R, et al. Superconductivity in single-crystalline aluminum- and gallium-hyperdoped germanium. *Phys Rev Mater*, 2019, 3, 054802
- [9] Wang M, Berencén Y, García-Hemme E, et al. Extended infrared photoresponse in Te-hyperdoped Si at room temperature. *Phys Rev Appl*, 2018, 10, 024054
- [10] Liu F, Prucnal S, Berencén Y, et al. Realizing the insulator-to-metal transition in Se-hyperdoped Si via non-equilibrium material processing. *J Phys D*, 2017, 50, 415102
- [11] Ziegler J F, Ziegler M D, Biersack J B. SRIM-The stopping and range of ions in matter (2010). *Nucl Instrum Methods Phys Res Sect B*, 2010, 268, 1818
- [12] Zhou S, Chen X L. Defect-induced magnetism in SiC. *J Phys D*, 2019, 52, 393001
- [13] Lee P A, Ramakrishnan T V. Disordered electronic systems. *Rev Mod Phys*, 1985, 57, 287
- [14] Pantelides S T. The electronic structure of impurities and other point defects in semiconductors. *Rev Mod Phys*, 1978, 50, 797
- [15] Park J, Choi J H, Kong K, et al. Electrically driven mid-submicrometre pixelation of InGaN micro-light-emitting diode displays for augmented-reality glasses. *Nat Photonics*, 2021, 15, 449
- [16] Zhou S, Li L, Yuan Y, et al. Precise tuning of the Curie temperature of (Ga, Mn)As-based magnetic semiconductors by hole compensation: Support for valence-band ferromagnetism. *Phys Rev B*, 2016, 94, 075205
- [17] Xu C, Wang M, Yuan Y, et al. Hole compensation effect in III-Mn-V dilute ferromagnetic semiconductors. *J Phys D*, 2019, 52, 355301
- [18] Rischau C W, Leridon B, Fauqué B, et al. Doping of Bi₂Te₃ using electron irradiation. *Phys Rev B*, 2013, 88, 205207
- [19] Liu Y, Li Z, Guo L, et al. Towards diluted magnetism in TaAs. *Phys Rev Mater*, 2017, 1, 044203
- [20] Hazdra P, Popelka S, Schöner A. Optimization of SiC power p-i-n diode parameters by proton irradiation. *IEEE Trans Electron Devices*, 2018, 65, 4483
- [21] Sharma R K, Hazdra P, Popelka S. The effect of light ion irradiation on 4H-SiC MPS power diode characteristics: Experiment and simulation. *IEEE Trans Nucl Sci*, 2015, 62, 534
- [22] Aspar B, Bruel M, Moriceau H, et al. Basic mechanisms involved in the Smart-Cut® process. *Microelectron J*, 1997, 36, 233
- [23] Bruel M, Aspar B, Auberton-Hervé A J. Smart-Cut: A new silicon on insulator material technology based on hydrogen implantation and wafer bonding. *Jpn Appl Phys*, 1997, 36, 1636
- [24] Dietl T, Ohno H, Matsukura F, et al. Zener model description of ferromagnetism in zinc-blende magnetic semiconductors. *Science*, 2000, 287, 1019
- [25] Y Yuan, T Amarouche, C Xu, et al. Switching the uniaxial magnetic anisotropy by ion irradiation induced compensation. *J Phys D*, 2018, 51, 145001
- [26] Dobrowolska M, Tivakornasithorn K, Liu X, et al. Controlling the Curie temperature in (Ga, Mn)As through location of the Fermi level within the impurity band. *Nat Mater*, 2012, 11, 444
- [27] Goennenwein S T B, Wassner T A, Huebl H, et al. Hydrogen control of ferromagnetism in a dilute magnetic semiconductor. *Phys Rev Lett*, 2004, 92, 227202
- [28] Sinnecker E H C P, Penello G M, Rappoport T G, et al. Ion-beam modification of the magnetic properties of Ga_{1-x}Mn_xAs epilayers. *Phys Rev B*, 2010, 81, 245203
- [29] Kudrawiec R. Conduction and valence band positions versus the Fermi-level stabilization energy in quaternary dilute nitrides. *Phys Status Solidi C*, 2011, 8, 1650
- [30] Wang C, Chang C H, Huang A, et al. Tunable disorder and localization in the rare-earth nickelates. *Phys Rev Mater*, 2019, 3, 053801
- [31] Evers F, Mirlin A D. Anderson transitions. *Rev Mod Phys*, 2008, 80,

- 1355
- [32] Smylie M P, Claus H, Kwok W K, et al. Superconductivity, pairing symmetry, and disorder in the doped topological insulator $\text{Sn}_{1-x}\text{In}_x\text{Te}$ for $x > 0.10$. *Phys Rev B*, 2018, **97**, 024511
- [33] Harimohan V, Bharathi A, Rajaraman R, et al. Magneto-resistance in pristine and irradiated TaAs_2 . *AIP Adv*, 2019, **9**, 045020
- [34] Shoenberg D. Magnetic oscillations in metals. Cambridge University Press, Cambridge, 1984
- [35] Hashibon A, Elsässer C. First-principles density functional theory study of native point defects in Bi_2Te_3 . *Phys Rev B*, 2011, **84**, 144117
- [36] Pecheur P, Toussaint G. Tight-binding studies of crystal stability and defects in Bi_2Te_3 . *J Phys Chem Solids*, 1994, **55**, 327
- [37] Chaudhari P, Bever M B. Effects of irradiation with protons on the electrical properties of Bi_2Te_3 . *J Appl Phys*, 1966, **37**, 4181
- [38] Chaudhari P, Bever M B. Defects in the compound Bi_2Te_3 caused by irradiation with protons. *J Appl Phys*, 1967, **38**, 2417
- [39] Smylie M P, Willa K, Claus H, et al. Robust odd-parity superconductivity in the doped topological insulator $\text{Nb}_x\text{Bi}_2\text{Se}_3$. *Phys Rev B*, 2017, **96**, 115145
- [40] Kimoto T, Cooper J A. Fundamentals of silicon carbide technology. Singapore: Wiley, 2014
- [41] Vobecký J, Hazdra P, Záhlava V, et al. ON-state characteristics of proton irradiated 4H-SiC Schottky diode: The calibration of model parameters for device simulation. *Solid-State Electron*, 2014, **94**, 32
- [42] Vobecký J, Hazdra P, Sharma S, et al. Impact of electron irradiation on the On-state characteristics of a 4H-SiC JBS diode. *IEEE Trans Electron Devices*, 2015, **62**, 1964
- [43] Hiyoji T, Kimoto T. Reduction of deep levels and improvement of carrier lifetime in n-type 4H-SiC by thermal oxidation. *Appl Phys Express*, 2009, **2**, 041101
- [44] Hazdra P, Popelka S, Záhlava V, et al. Radiation damage in 4H-SiC and its effect on power device characteristics. *Solid State Phenomena*, 2015, **242**, 421
- [45] Williams J S. Ion implantation of semiconductors. *Mater Sci Eng A*, 1998, **253**, 8
- [46] Hallén A, M S Janson, YuKuznetsov A, et al. Ion implantation of silicon carbide. *Nucl Instrum Methods Phys Res Sect B*, 2002, **186**, 186
- [47] Zolper J C. Ion implantation in group III-nitride semiconductors: a tool for doping and defect studies. *J Crys Growth*, 1997, **178**, 157
- [48] Pearson S J. Ion implantation in III-V semiconductor technology. *Int J Mod Phys B*, 1993, **7**, 4687
- [49] Alfieri G, Monakhov E V, Svensson B G, et al. Annealing behavior between room temperature and 2000 °C of deep level defects in electron-irradiated n-type 4H silicon carbide. *J Appl Phys*, 2005, **98**, 043518
- [50] Zippelius B, Suda J, Kimoto T. High temperature annealing of n-type 4H-SiC: Impact on intrinsic defects and carrier lifetime. *J Appl Phys*, 2012, **111**, 033515
- [51] Dalibor T, Pensl G, Matsunami H, et al. Deep defect centers in silicon carbide monitored with deep level transient spectroscopy. *Phys Status Solidi A*, 1997, **162**, 199
- [52] Klein P B, Shanabrook B V, Huh S W, et al. Lifetime-limiting defects in n- 4H-SiC epilayers. *Appl Phys Lett*, 2006, **88**, 052110
- [53] Pintilie I, Pintilie L, Irmscher K, et al. Formation of the $Z_{1,2}$ deep-level defects in 4H-SiC epitaxial layers: Evidence for nitrogen participation. *Appl Phys Lett*, 2002, **81**, 4841
- [54] Eberlein T A G, Jones R, Briddon P R. Z_1/Z_2 defects in 4H-SiC. *Phys Rev Lett*, 2003, **90**, 225502
- [55] Storasta L, Henry A, Bergman J P, et al. Investigations of possible nitrogen participation in the Z_1/Z_2 defect in 4H-SiC. *Mater Sci Forum*, 2004, **457-460**, 469
- [56] Storasta L, Tsuchida H. Reduction of traps and improvement of carrier lifetime in epilayers by ion implantation. *Appl Phys Lett*, 2007, **90**, 062116
- [57] Storasta L, Tsuchida H, Miyazawa T. Enhanced annealing of the $Z_{1/2}$ defect in 4H-SiC epilayers. *J Appl Phys*, 2008, **103**, 013705
- [58] Ichikawa S, Kawahara K, Suda J, et al. Carrier recombination in n-type 4H-SiC epilayers with long carrier lifetimes. *Appl Phys Express*, 2012, **5**, 101301
- [59] Hazdra P, Popelka S, Schöner A. Local lifetime control in 4H-SiC by proton irradiation. *Mater Sci Forum*, 2018, **924**, 436
- [60] Achtinger N, Pasold G, Sielemann R, et al. Tungsten in silicon carbide: Band-gap states and their polytype dependence. *Phys Rev B*, 2000, **62**, 12888
- [61] Hemmingsson C, Son N T, Kordina O, et al. Deep level defects in electron-irradiated 4H SiC epitaxial layers. *J Appl Phys*, 1997, **81**, 6155
- [62] Storasta L, Bergman J P, Janzén E, et al. Deep levels created by low energy electron irradiation in 4H-SiC. *J Appl Phys*, 2004, **96**, 4909
- [63] Hazdra P, Popelka S. Lifetime control in SiC PiN diodes using radiation defects. *Mater Sci Forum*, 2017, **897**, 463
- [64] Son N T, Trinh X T, Løvlie L S, et al. Negative-U system of carbon vacancy in 4H-SiC. *Phys Rev Lett*, 2012, **109**, 187603
- [65] Vobecký J, Hazdra P, Záhlava V. Open circuit voltage decay lifetime of ion irradiated devices. *Microelectron J*, 1999, **30**, 513
- [66] Guerrero P, Sanseverino A, Daliento S. Lifetime profile reconstruction in helium implanted silicon for planar IGBTs. 29th International Conference on Microelectronics Proceedings - MIEL 2014, Belgrade, 2014, 325
- [67] Hazdra P, Brand K, Rubeš J, et al. Local lifetime control by light ion irradiation: impact on blocking capability of power P-i-N diode. *Microelectron J*, 2001, **32**, 449
- [68] Napoli E, Strollo A G M, Spirito P. Numerical analysis of local lifetime control for high-speed low-loss P-i-N diode design. *IEEE Trans Power Electron*, 1999, **14**, 615
- [69] Hazdra P, Komarnitskyy V. Lifetime control in silicon power P-i-N diode by ion irradiation: Suppression of undesired leakage. *Microelectron J*, 2006, **37**, 197
- [70] Kohno I. Production of fast-switching power thyristors by proton irradiation. *Nucl Instrum Methods Phys Res Sect B*, 1989, **37/38**, 739
- [71] Sawko D C, Bartko J. Production of fast switching power thyristors by proton irradiation. *IEEE Trans Nucl Sci*, 1983, **30**, 1756
- [72] Hazdra P, Brand K, Vobecký J. Effect of defects produced by MeV H and He ion implantation on characteristic of power silicon P-i-N diodes. 2000 International Conference on Ion Implantation Technology, 2000, 135
- [73] Hazdra P, Vobecký J, Dorschner H, et al. Axial lifetime control in silicon power diodes by irradiation with protons, alphas, low- and high-energy electrons. *Microelectron J*, 2004, **35**, 249
- [74] Hazdra P, Rubeš J, Vobecký J. Divacancy profiles in MeV helium irradiated silicon from reverse I-V measurement. *Nucl Instrum Methods Phys Res Sect B*, 1999, **159**, 207
- [75] Vobecký J, Hazdra P, Záhlava V. Helium irradiated high-power P-i-N diode with low On-state voltage drop. *Solid-State Electron*, 2003, **47**, 45
- [76] Vobecký J, Hazdra P. The application of platinum-silicide anode layer to decrease the static and turn-off losses in high-power P-i-N diode. *Thin Solid Films*, 2003, **433**, 305
- [77] Vobecký J, Hazdra P. Advanced local lifetime control for higher reliability of power devices. *Microelectron Reliab*, 2003, **42**, 1883
- [78] Prabhakar A, McGill T C, Nicolet M A. Platinum diffusion into silicon from PtSi. *Appl Phys Lett*, 1983, **43**, 1118
- [79] Schmidt D C, Svensson G, Godey S, et al. The influence of diffusion temperature and ion dose on proximity gettering of platinum in silicon implanted with alpha particles at low doses. *Appl Phys Lett*, 1999, **74**, 3329
- [80] Seol D, Kim S, Jang W S, et al. Selective patterning of out-of-plane piezoelectricity in MoTe_2 via focused ion beam. *Nano Energy*,

2021, 79, 105451

- [81] Mitterreiter E, Schuler B, Cochrane K A, et al. Atomistic positioning of defects in helium ion treated single-layer MoS₂. *Nano Lett.*, 2020, 20, 4437
- [82] Babin C, Stöhr R, Morioka N, et al. Fabrication and nanophotonic waveguide integration of silicon carbide colour centres with preserved spin-optical coherence. *Nat Mater.*, 2022, 21, 67
- [83] Kasper C, Klenkert D, Shang Z, et al. Influence of irradiation on defect spin coherence in silicon carbide. *Phys Rev Appl.*, 2020, 13, 044054
- [84] Bathen M E, Vines L. Manipulating single-photon emission from point defects in diamond and silicon carbide. *Adv Quantum Technol.*, 2021, 4, 2100003
- [85] Xiong W, Zhou X, Xu G, et al. Double-barrier-Ga₂O₃ Schottky barrier diode with low turn-on voltage and leakage current. *IEEE Electron Device Lett.*, 2021, 42, 430
- [86] He Q, Hao W, Zhou X, et al. Over 1 GW/cm² vertical Ga₂O₃ Schottky barrier diodes without edge termination. *IEEE Electron Device Lett.*, 2022, 43, 264
- [87] Hao W, He Q, Zhou K, et al. Low defect density and small curve hysteresis in NiO/β-Ga₂O₃ pn diode with a high PFOM of 0.65 GW/cm². *Appl Phys Lett.*, 2021, 118, 043501
- [88] Hou X, Zhao X, Zhang Y, et al. High-performance harsh-environment-resistant GaO_x solar-blind photodetectors via defect and doping engineering. *Adv Mater.*, 2022, 34, 2106923



Ye Yuan got his BS and MS degrees from the Harbin Institute of Technology in 2011 and 2013, respectively. Afterwards, he got a PhD from Technische Universität Dresden in 2017. Then he joined Helmholtz-Zentrum Dresden-Rossendorf and King Abdullah University of Science and Technology as postdoc in 2017 and 2018, respectively. In 2019, he joined Songshan Lake Materials Laboratory as an associate investigator. His research mainly focuses on the growth and physics in wide bandgap semiconductors, as well as the application of ion beam in semiconductors.



Shengqiang Zhou is the “Semiconductor Materials” department head at Helmholtz-Zentrum Dresden-Rossendorf, Germany. He got his BSc and MSc degree from Peking University and PhD degree from Technische Universität Dresden. His current research interests include III-V:Mn magnetic semiconductors synthesized by ion implantation and pulsed laser annealing, hyperdoing semiconductors by ion implantation, defect engineering by ion irradiation and ion beam analysis. As the principal investigator, he has acquired 4 DFG projects and 3 Helmholtz Association Research Programs.



Xinqiang Wang is a full Professor of School of Physics at Peking University. He joined the faculty on May 2008, after more than 6 years' postdoctoral research at Chiba University and Japan Science Technology Agency, Japan. He has received the China National Funds for Distinguished Young Scientists in 2012 and has been awarded Changjiang Distinguished Professor by Ministry of Education in 2014. He mainly concentrates on III-nitrides compound semiconductors including epitaxy and device fabrication. He is the author or co-author of 200+ refereed journal articles with over 3800 citations and has delivered over 40 invited talks at scientific conferences and contributed three chapters in three books.